~~SECRET~~

SRI International

Special Technical Report 2

29 January 1980

VELA METEOROID EVALUATION (U)

Short Title: T/8503/T/PMP (U)

By: GEORGE N. OETZEL STEVEN C. JOHNSON

Prepared for:

AIR FORCE TECHNICAL
APPLICATIONS CENTER
PATRICK AIR FORCE BASE
FLORIDA 32925

SRI Project 6914

Contract No: F08606-78-C-0012
AFTAC Project Authorization No:
T/8503
Date of Contract:
21 October 1977
Contract Expiration Date:
30 September 1980
Amount of Contract: $190,657
Project Scientist: G. N. Oetzel
Telephone: (415) 326-6200
Ext. 3782

Approved by:

WALTER E. JAYE, *Project Supervisor*
Radio Physics Laboratory

ROBERT S. LEONARD, *Director*
Radio Physics Laboratory

ORIGINAL CLASSIFICATION
CANCELLED OR DOWNGRADED
TO Unclassified/Full Release
AUTHORITY FOIA 552(b)
BY AFTAC/dlw DATE 29 Jan 01

Copy No. 4

This document consists of 50 pages.

SRI 0-4055

CLASSIFIED BY DD Form 254, dated
7 August 1978, F08606-78-C-0012
REVIEW ON: 29 January 2000

~~SECRET~~

333 Ravenswood Ave. • Menlo Park, California 94025
(415) 326-6200 • Cable: SRI INTL MPK • TWX: 910-373-1246

THIS PAGE BLANK

CONTENTS (U)

ILLUSTRATIONS (U)

TABLES (U)

I INTRODUCTION (U)

(S) This report describes the results of a brief, intensive effort to assess the probability that the optical signal obtained by the VELA 6911 spacecraft on 22 September 1979 (also known as Event 747) was actually produced by sunlight reflected from a meteoroid. This study was conducted under a severe time constraint. We were given only three weeks from the time when we received the Neste (1974) thesis containing the unprocessed Pioneer 10 data until the finished report was due. For the bulk of the VELA unexplained data (the VELA "zoo") the time was less than one week.

(S) Prior studies by MRC (Sappenfield, 1979) and Sandia (Mauth, 1979) developed several meteoroid shape and trajectory models that could explain the observed waveforms. One of the central issues in these studies was an explanation of the differences between the time histories obtained by the "YC" and "YV" sensors on the spacecraft.

(S) We were asked in December, 1979 to perform a quick, preliminary assessment of the probability that the circumstances postulated in these models would occur in 120 sensor-years of bhangmeter observations. Meteoroid flux data contained in a review article by Dohnanyi (1972) indicated that they were extremely improbable and could be discounted as possible explanations for Event 747. Following this preliminary study, our attention was directed to the Pioneer 10 optical meteoroid detection experiment in which many more detections were observed than our analysis would have predicted. We were asked to perform and report on the following tasks:

1. Conduct a thorough literature survey to incorporate all relevant data into the flux and velocity distributions used in our analysis.
2. Compare the Pioneer 10 data with the VELA "zoo" (a set of unexplained observations from the VELA bhangmeters).
3. Re-evaluate the MRC and Sandia models as possible explanations for Event 747.

(U) The accepted meteoroid flux distribution used in our preliminary analysis is supported by a large number of ground-and space-based observations. Further measurements since the 1972 Dohnanyi article have not undermined this distribtuion. Rather, they have added data about the population of extremely small particles that are not of interest for the present problem.

(U) In this framework of mutually reinforcing observations, the Pioneer 10 AMD (Asteroid/Meteoroid Detector) stands as a unique and puzzling experiment. When the data are reduced in straightforward fashion, the resulting distribution of particle sizes is substantially in disagreement with all other measurements. There is no indication that the instruments failed to work as intended. There is every reason to believe that the AMD reported valid optical observations. What is lacking is a satisfactory model that reproduces the particle mass statistics and AMD observations simultaneously. One proposed model ascribes many of the detections to specular surfaces on meteoroids.

(U) Since valid optical observations are superior to an inadequate theory about how they are produced, we regard the Pioneer 10 data as the most relevant set of data to apply to the VELA problem. The AMD is quite similar to the VELA bhangmeter; if one device experiences an unexpected optical environment, it is likely that the other one will also. Thus, we have concluded that the raw, uninterpreted Pioneer 10 data are the only external data that can be compared meaningfully with the VELA data without involving a number of unsupportable assumptions.

(U) This report is organized as follows. The literature search is summarized in Chapter II. In Chapter III, we use the accepted data base for meteoroid flux and velocity distributions to evaluate the MRC and Sandia models. In Chapter IV, we describe the Pioneer 10 experiment and show that the data from this experiment are not consistent with the calculations based on the accepted data base. Chapter V is a discussion of the VELA "zoo," with particular emphasis on the time histories, which have no counterpart in the AMD results. In Chapter VI, the VELA data

(U)
are reduced to a form comparable with the Pioneer data so that their similarities and differences can be examined. Our conclusions are given in Chapter VII.

II LITERATURE SURVEY (U)

(U) A literature search was conducted to incorporate any new, pertinent information into the data base used in our preliminary analysis (the preliminary data base came from Dohnanyi, 1972). This search relied heavily on the extensive reference list contained in a review article by Brownlee (1979) and on two books: Cosmic Dust (J.A.M. McDonnell, ed., Wiley, 1978) and Lecture Notes in Physics 48: Interplanetary Dust and Zodiacal Light (Elsässer and Fechtig, eds., Springer-Verlag, 1976). The search concentrated on four categories of meteoroid data:

- flux versus size data
- velocity data (direction and magnitude)
- rotation rate data
- meteoroid cluster or swarm data.

These categories are discussed in detail below.

A. Meteoroid Size Distribution (U)

(U) Dohnanyi (1972) contains a graph of the cumulative influx of particles into the earth's atmosphere as a function of particle mass M. Combining data from over a dozen different studies, this graph comprises data from a mass range of

$$10^{-13} \leq M(kg) \leq 10^{10} .$$

Most recent studies have involved highly sensitive spacecraft-mounted sensors that respond to very small particle masses ($10^{-20} < M(kg) < 10^{-12}$). These measurements, summarized in Table 1 (from Bedford et al., 1975), fall in the upper left hand corner of Dohnanyi's graph as shown in Figure 1.

Table 1

(U) NEAR EARTH AND INTERPLANETARY METEOROID FLUXES

(FROM BEDFORD ET AL., 1975) (U)

Experiment	Technique	Region of Space and Orbital Data (a)	Mass Threshold (gm)	Cumulative Flux $(m^{-2}s^{-1}(2\pi sr)^{-1})$	Reference
NEAR EARTH					
Prospero	Impact	Geocentric	2×10^{-15}	4×10^{-1}	Bedford et al., (1975)
	Ionization	6,900-7,900 km	6×10^{-15}	1.4×10^{-1}	
			2×10^{-14}	1.4×10^{-2}	
HEOS	Impact	Geocentric	$\sim 10^{-15}$	4×10^{-2} (b)	Hoffman et al., (1974)
	Ionization	6,700-67,000 km	$\sim 10^{-14}$	3×10^{-2} (b)	
Cosmos 470		Geocentric	1×10^{-11}	2×10^{-3}	Nazarova and Rybakov (1974)
Cosmos 502		"	1×10^{-11}	2×10^{-3}	
InterCosmos 6		"	1×10^{-9}	8×10^{-5}	
INTERMEDIATE					
OGO III	Penetration/ Piezoelectric	Geocentric 10,000-100,000 km	2×10^{-13}	2×10^{-3}	Alexander et al., (1973)
INTERPLANETARY					
HEOS	Impact	Geocentric	$\sim 10^{-15}$	$\sim 4 \times 10^{-3}$ (b)	Hoffman et al., (1974)
	Ionization	67,000-246,400 km	$\sim 10^{-14}$	8×10^{-4} (b)	
			1.0^{-12}	4×10^{-4} (c)	
			10^{-12}	$\sim 4 \times 10^{-5}$ (d)	
Pioneer 8 and Pioneer 9	Impact	Heliocentric	1×10^{-13}	1×10^{-3}	McDonnel, Berg and Richardson (1975)
	Ionization	1 AU	to 1×1^{-11}	to 4×10^{-5}	
Mariner IV	Penetration/	Heliocentric	6×10^{-12}	1×10^{-4}	Alexander and Bohn (1974)
	Piezoelectric	1.0 - 1.5 AU	to 2×10^{-10}	to 2×10^{-5}	
IE 35	Piezoelectric/	Selenocentric	5×10^{-12}	2×10^{-4}	Alexander et al., (1973)
	Capacitor	2,000-9,000 km	1×10^{-10}	7×10^{-6}	
Luna 19	Piezoelectric/ Capacitor	Selenocentric	1×10^{-10}	2×10^{-5}	Nazarova and Rybakov (1974)
Lunar Craters	Microcrater	Lunar Surface	1×10^{-14}	$\sim 10^{-3}$ (e)	Smith et al., (1974)
	Analysis		1×10^{-12}	2×10^{-5}	
			1×10^{-10}	2×10^{-6}	
			1×10^{-16}	3×10^{-3}	Fechtig et al., (1973)
			to 1×10^{-10}	to 2×10^{-6}	
Pioneer 10(f)	Penetration	Interplanetary 1-2 AU	2×10^{-9}	1×10^{-5}	Humes et al., (1974)

(a) references to the centre of the parent body
(b) values calculated by us from published data
(c) flux from the Earth's apex direction
(d) flux from all other directions
(e) extrapolated value using Smith et al data for high density (~ 8 gm cm^{-3}) micrometeoroids
(f) added to the original table for this report.

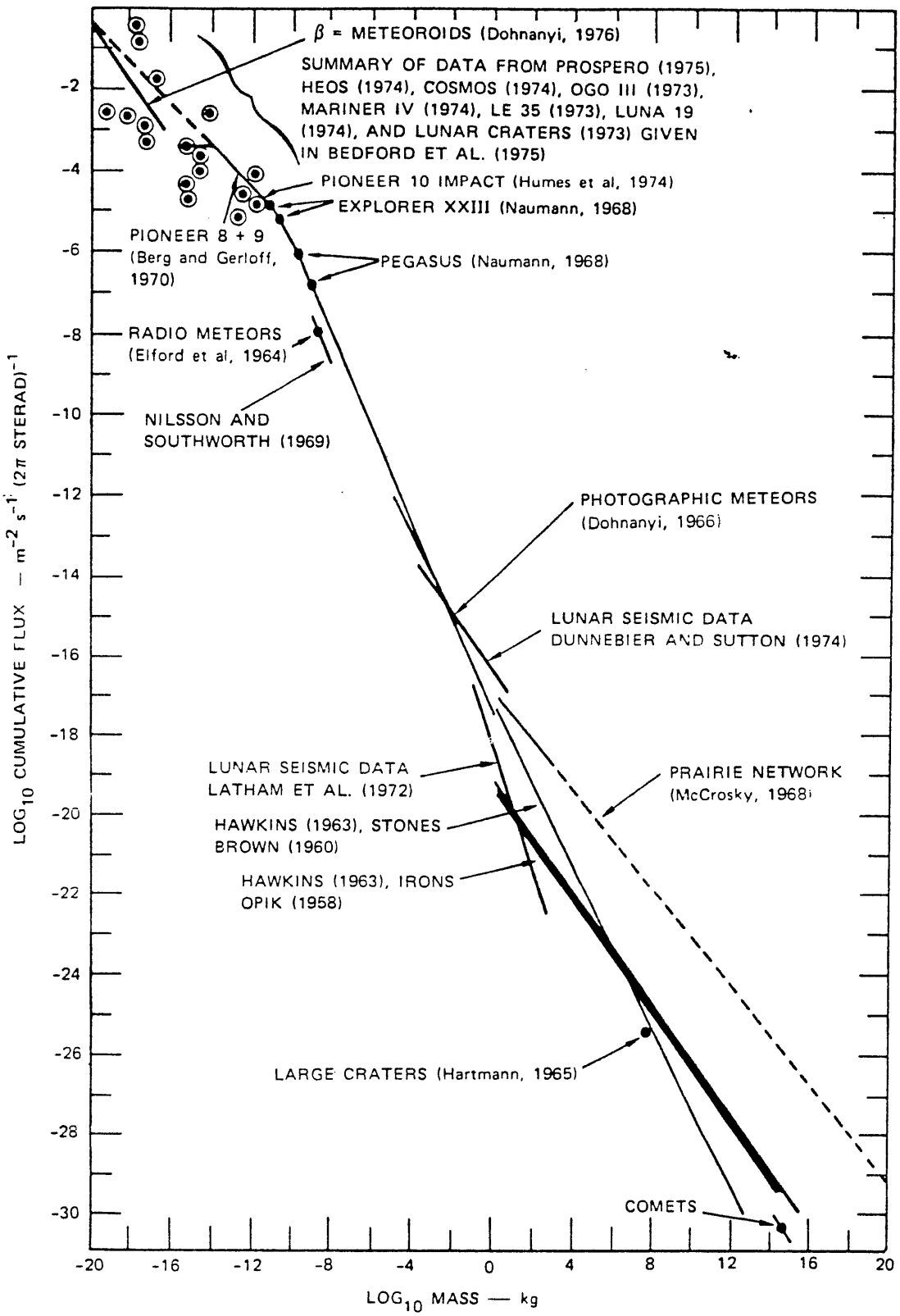

FIGURE 1 METEOROID FLUX DISTRIBUTION (U)

(U) The only other significant additions to Dohnanyi's plot are the data on lunar meteoroid impacts from the Apollo 14 lunar seismic station (Latham et al., 1972; Dunnebier and Sutton, 1974). These are shown in the central portion of Figure 1. Note that in the mass region of interest to this analysis ($10^{-9} \leq M(kg) \leq 10^{-3}$), the curve in Figure 1 can be approximated by

$$F(m) = 3.16 \times 10^{-18} m^{-1.18} \quad .$$

(U) All flux measurement results published since 1972 are in good agreement with the curve in Figure 1 except for the results of the optical meteoroid sensor on Pioneer 10 (Soberman et al., 1974). Questions have been raised regarding the interpretation and reduction of this data (Auer, 1976), and there is now general agreement in the community that this data is due to glints (Soberman, 1976; McDonnell, 1978; Cook, 1978; Dohnanyi, 1978). If this interpretation is correct, it is impossible to relate the Pioneer 10 optical data to actual particle sizes. The Pioneer 10 optical data are discussed in detail in a later section.

(U) The curve in Figure 1 represents the best current estimate of the meteoroid flux distribution. The principal unresolved area relating to size and mass distributions is with regard to the density of individual particles. Density values ranging from 0.18 gm/cm^3 (Cook, 1968) to 8 gm/cm^3 (Bedford et al., 1975) have been used, although values of 1-2 gm/cm^3 are most common. As a consequency, there is still an uncertainty (of about 1.5 orders of magnitude) in the mass-to-size relationship of meteoroids.

B. Meteoroid Velocities (U)

(U) The distribution of meteoroid velocities is not nearly as well documented as the mass distribution. Although much data exists on the velocity distribution of meteors, these data are distorted by several selection effects (e.g., low velocity meteors are more difficult to detect than high velocity meteors) and by the velocity increase

(U)
experienced as the meteor is accelerated by the earth's gravitational field. For example, Figure 2 shows the geocentric meteor velocity distributions for visual meteors and faint radio meteors (Hughes, 1978). In both cases, the lower limit of the distribution is given by the free-fall velocity (11.2 km/sec) of a particle hitting the earth that started with zero geocentric velocity at infinity.

(U) Another possible source of velocity data is the orbital parameters of observed meteors. Figure 3 is a summary of the parameters of several thousand radio and photographic meteor orbits (from Hughes, 1978). Although in theory these orbital parameter distributions can be transformed into a velocity distribution, it is not clear that the result would be any more believable than the distribution of Figure 2. After all, this orbital data is subject to the same selection processes operative on the data in Figure 2. For example, the almost total absence of low eccentricity orbits is possibly a result of these selection processes.

(U) An attempt to correct for these selection processes was made by Southworth and Sekanina (1973). Such a correction is similar to trying to multiply out a zero of a function without knowing the order (or even the nature) of the zero. The correction factor is inherently large and subject to large errors.

(U) The only velocity data extant on meteoroids was collected by Pioneers 8 and 9 (Gerloff and Berg, 1972; Wolf et al., 1976), and HEOS II (Hoffman et al., 1975). These data, shown in Figures 4 and 5 are all for particles of mass $< 10^{-8}$ gm ($< 10^{-9}$ gm for HEOS II); consequently they are at the extreme end of the mass range of interest for this analysis. Pioneer 8 and 9 data also indicated that the velocity distribution is anisotropic and somewhat mass dependent. In particular, these data show (McDonnell, 1978):

1) prograde orbits are preferred
2) masses $\geq 10^{-11}$ gm show apex symmetry (implying bound orbits)
3) smaller masses show apex asymmetry (i.e., are being blown out of the solar system by radiation pressure).

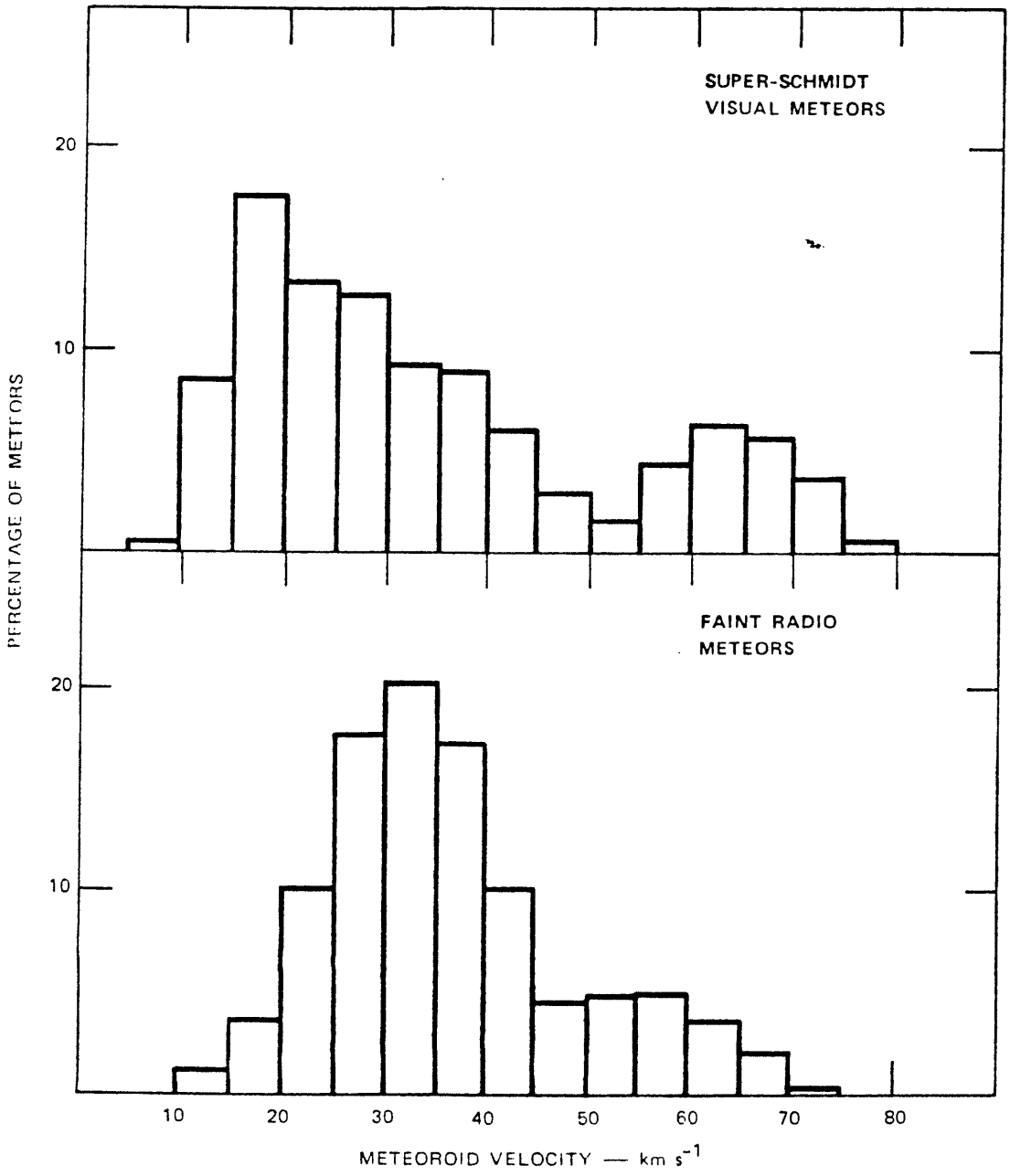

FIGURE 2 VELOCITY DISTRIBUTIONS OF VISUAL AND RADIO METEORS (U)

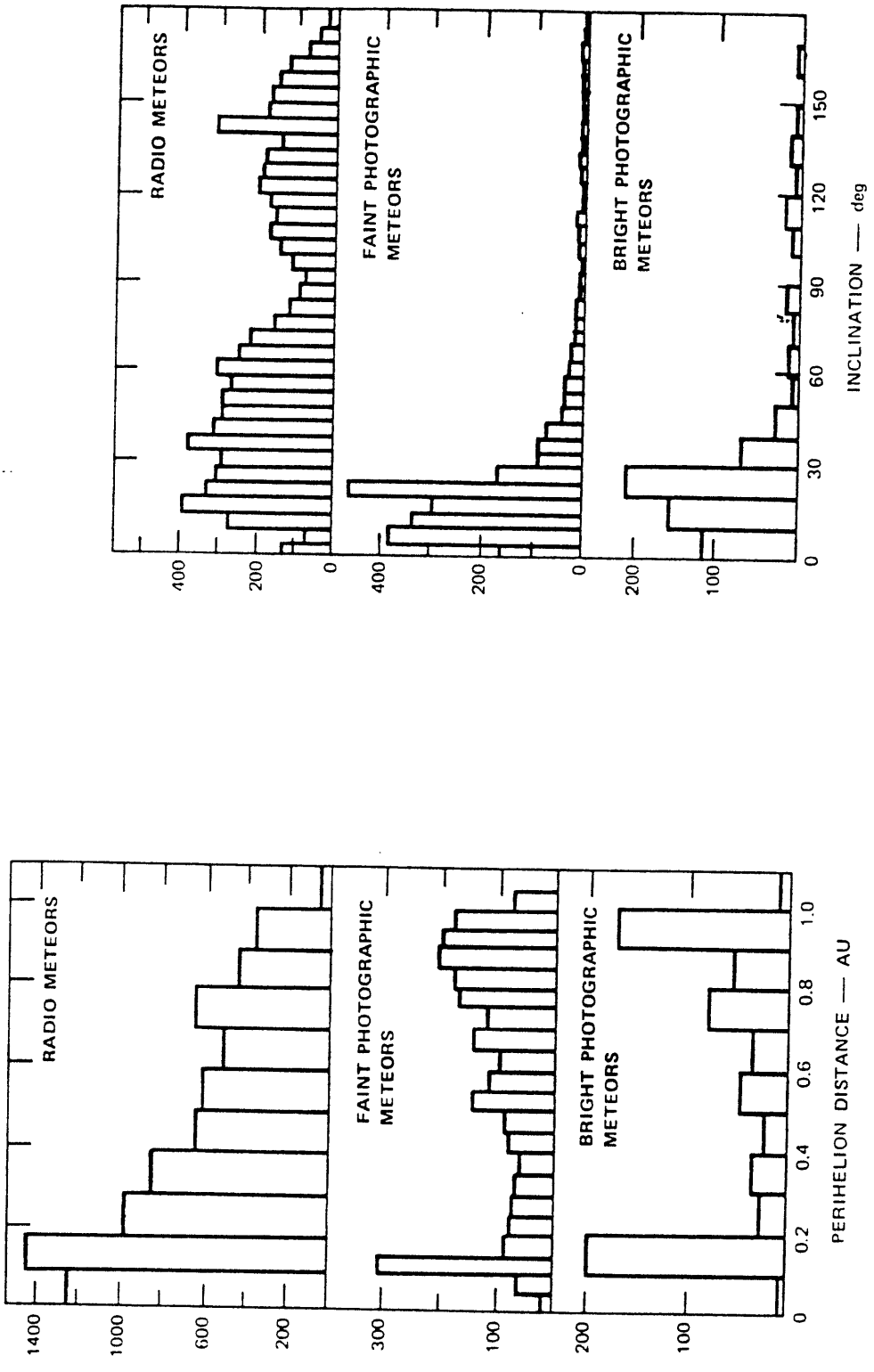

FIGURE 3 ORBITAL PARAMETERS OF METEORS (from Hughes, 1978) (U)

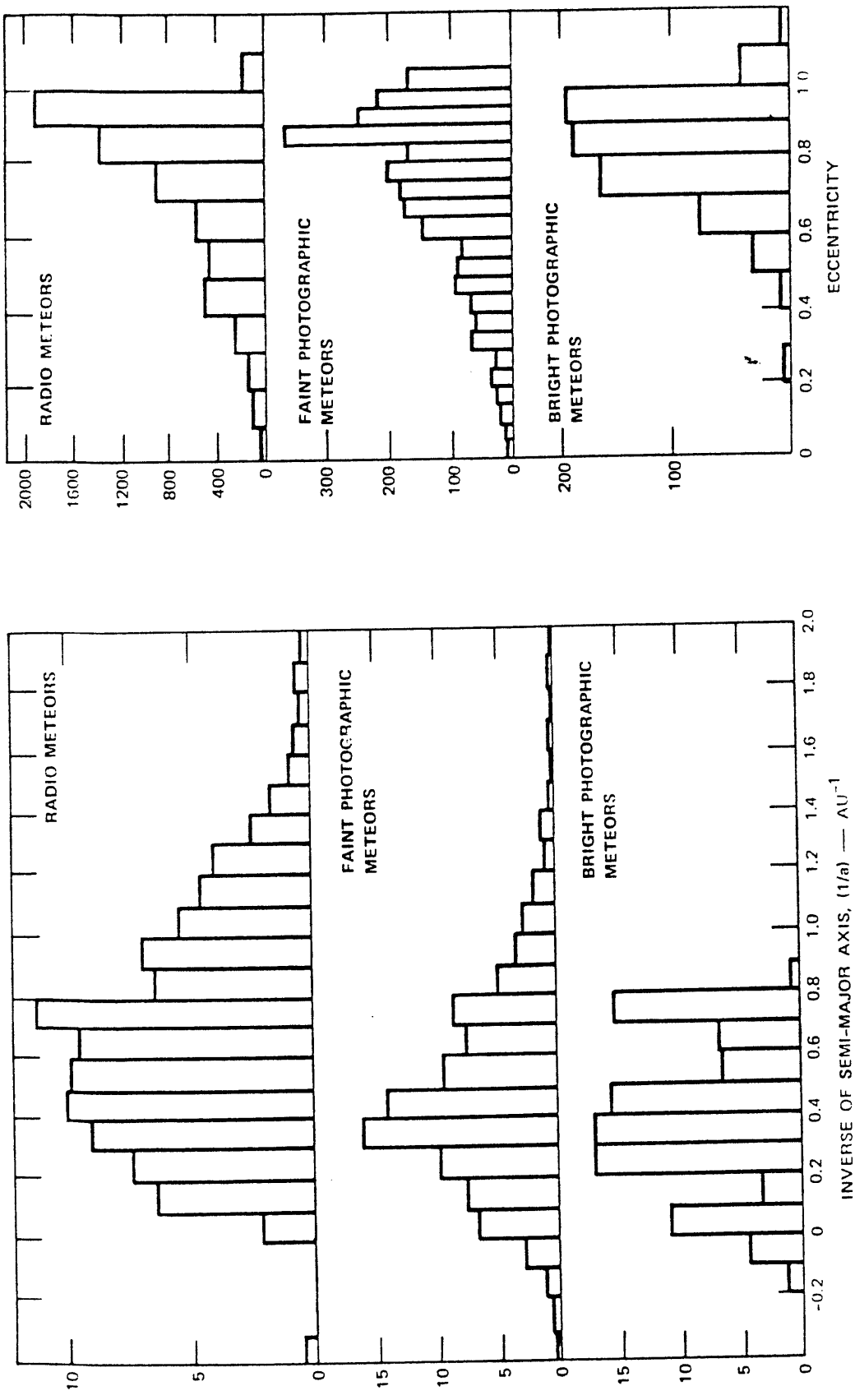

(b) SEMI-MAJOR AXIS AND ECCENTRICITY

FIGURE 3 (Concluded) (U)

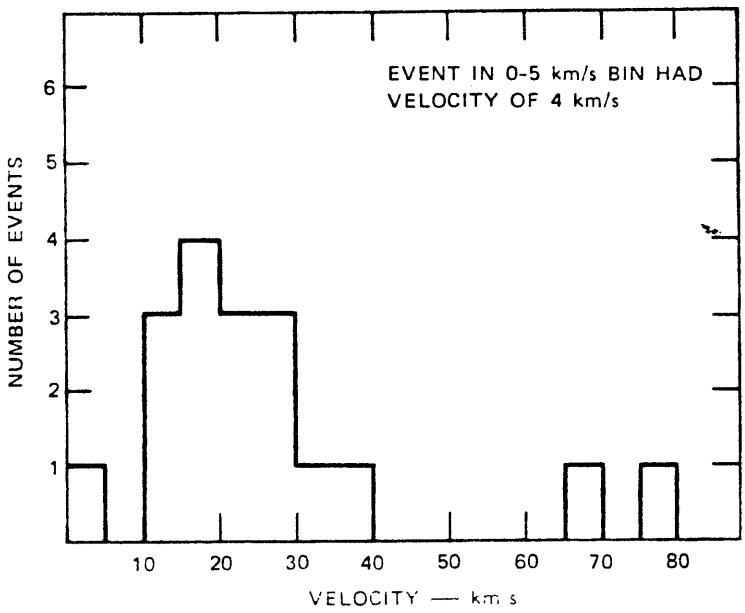

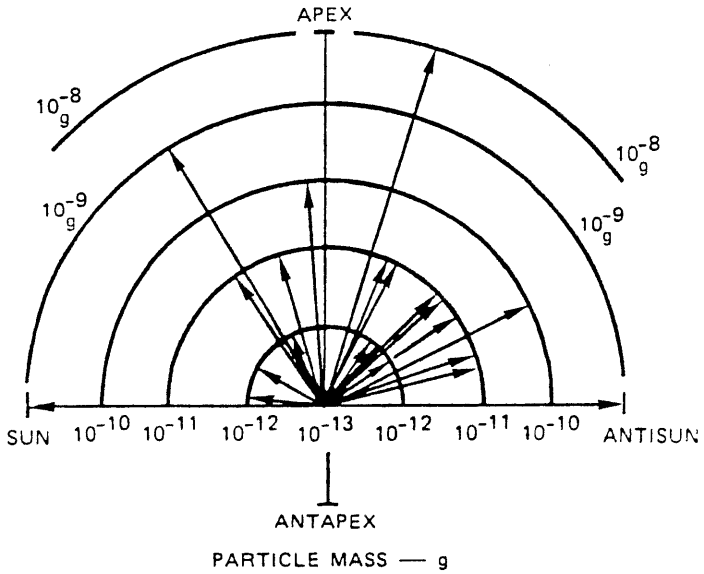

FIGURE 4 DISTRIBUTION OF VELOCITIES OF PARTICLES DETECTED BY PIONEERS 8 AND 9 (U)

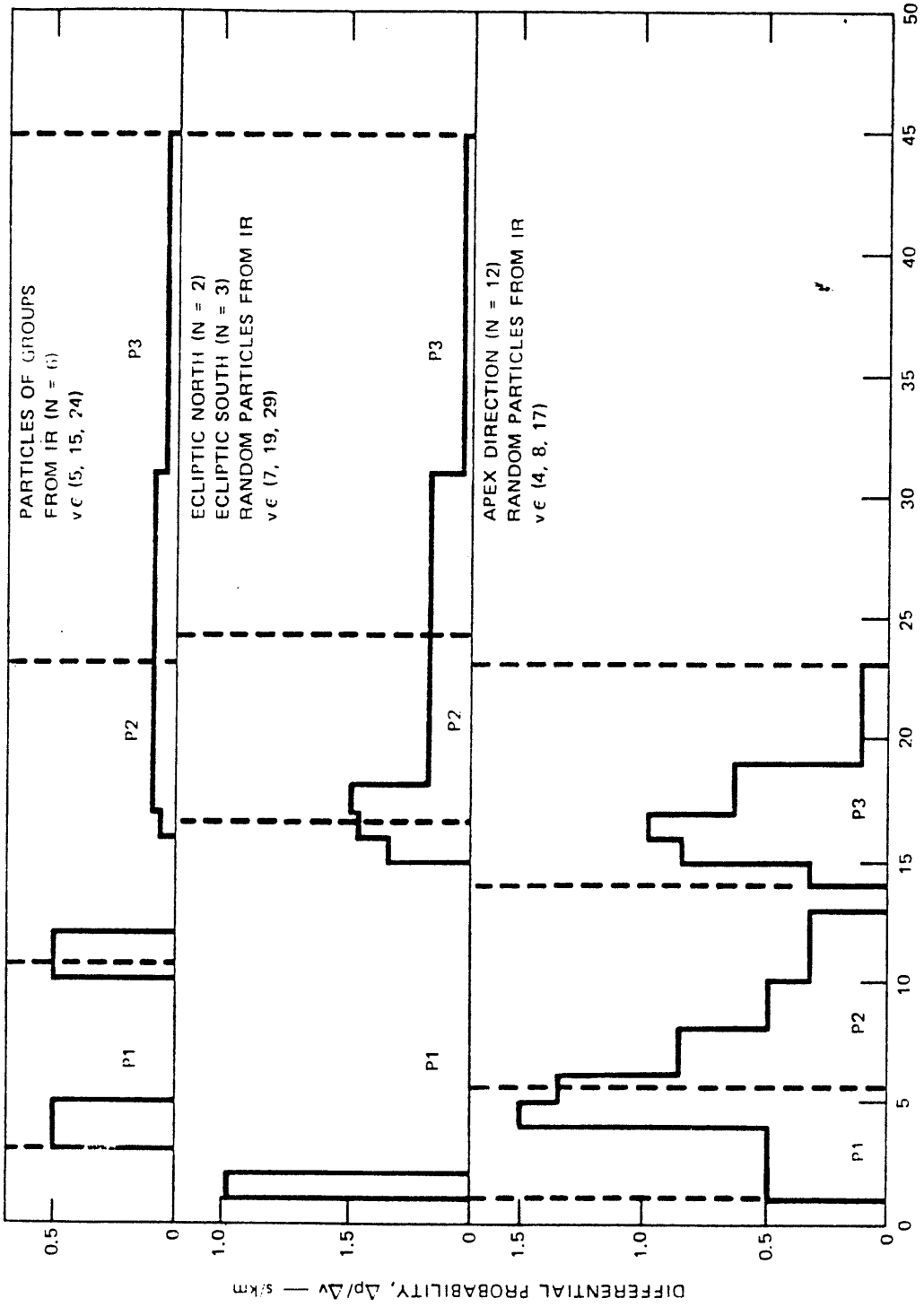

FIGURE 5 DISTRIBUTION OF SPEEDS OF PARTICLES DETECTED BY HEOS II (Hoffman et al., 1975) (U)

(U)

Since the majority of data collected by both the Pioneer sensors and HEOS is for particles of mass $\leq 10^{-11}$ gm, it is not clear that this data is applicable to particles in the mass range of our interest ($10^{-6} < M < 1.0$ gm). Furthermore, the distributions in Figures 4 and 5 represent very small sample sizes--20 detected particles for Pioneers 8 and 9 and 21 particles for HEOS II.

(U) An alternative to the distributions of Figures 4 and 5 is the meteor velocity distribution of Figure 2 transformed to make it applicable at 100,000 km. This is accomplished by subtracting the kinetic energy gain a particle realizes as it falls from 100,000 km to the surface of the earth. There is a serious problem with the transformation, however. At 100,000 km, the escape velocity is $\sim$ 2.8 km/sec and the circular orbit velocity is $\sim$ 2 km/sec. It is almost impossible for a particle that enters the earth's gravitational field at essentially infinity (which is the case with most meteoroids) to have a velocity less than 2.8 km/sec at 100,000 km. This leaves a gap of 800 m/sec between the slowest particle speed and VELA. The problem is that one of the meteoroid models for the VELA measurement (the MRC model) requires low particle velocities relative to VELA ($0 \leq |v| \leq 300$ m/sec). These low relative velocities will not occur unless a particle encounters some means of losing a portion of its kinetic energy, such as a brush with the earth's atmosphere or a collision with another object before encountering the VELA sensors. Although neither of these mechanisms is very likely, the transformation (up to 100,000 km) should reflect the fact that the probability of a particle having a velocity hear 2 km/sec is small but not zero. Data on which to estimate this probability does not exist, however, and any estimate we could make of the probability of a meteoroid-VELA encounter at relative velocities below 800 m/sec would be unsupportable.

C. Rotation (U)

(U) Rotation appears to be a universal attribute of astronomical bodies, hence it is reasonable to assume that meteoroids are rotating. Two mechanisms have been proposed to induce a state of rotation:

(U)

- Collisions (Dohnanyi, 1972; Zook and Berg, 1975)
- Radiation pressure combined with an asymmetrical shape (or albedo) or a symmetrical, but windmill like, shape. (Radzievsky, 1954; Paddock and Rhee, 1976).

Mechanisms for dissipating this rotational energy are weak or nonexistent, hence a particle's spin rate will tend to increase until the particle bursts due to excessive internal tensions. Dohnanyi (1976) has used random walk theory to analyze spin-up by collisions and has developed a density function for the spin rate given by

$$f_{\omega}(\omega)d\omega = \frac{15}{2} N \frac{\omega^2 (\omega_x^2 - \omega^2)}{\omega_x^5} d\omega$$

where $f_{\omega}(\omega)d\omega$ is the number of particles with spin rates between ω and $\omega + d\omega$, ω_x is the bursting spin rate, and N is the total number of particles. This expression is plotted in Figure 6 together with the distribution of rotation rates of known asteroids. Integration of the above expression from $0.1\ \omega_x$ to ω_x gives the result that over 99.7% of all particles are spinning at a rate between $0.1\ \omega_x$ and ω_x.

(U) For small particles, the bursting rate is much higher than asteroids, hence the average rotation rate will be greater. For example, a particle 2 mm in diameter, with a density of 2 gm/cm^3 and relatively low tensile strength, could spin up to 10^7 rotations per second before bursting. This stretches the right side of the theoretical curve in Figure 6 out to 10^7 and means that over 99% of all particles of this size (and smaller) are spinning faster than 10^6 rotations per second. It is difficult to reconcile these rapid spin rates with specular reflections lasting milliseconds or longer.

D. Meteoroid Clustering (U)

(U) The clustering of meteors into showers is a well-known fact (Hughes, 1978). Events within a shower, however, are usually separated by minutes or hours--not milliseconds. The tendency of micrometeoroids

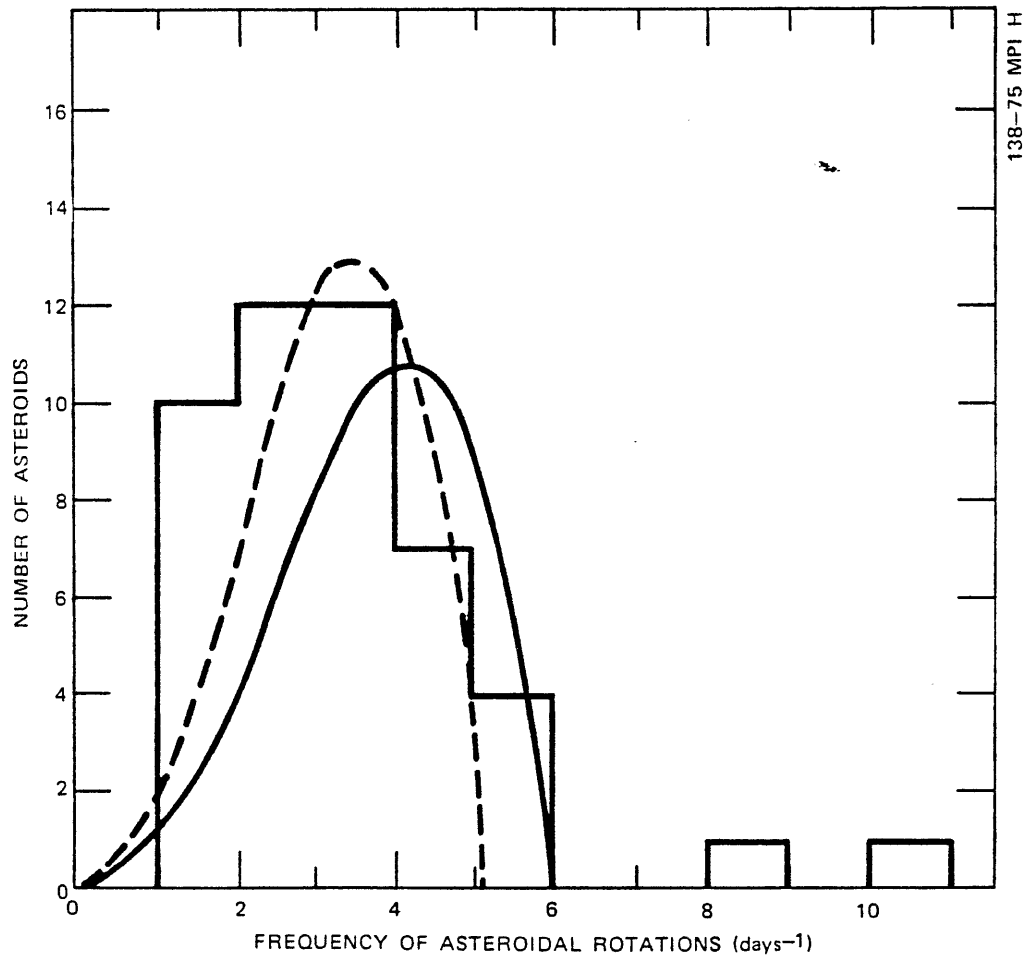

FIGURE 6 DISTRIBUTION OF ASTEROIDAL ROTATION RATES (U)

to cluster in time and space has been measured by HEOS II (Fechtig et al., 1979) and also found to be large. Figure 7 shows the temporal distribution of 431 detected particles of mass $\leq 10^{-9}$ gm detected below 60,000 km. This clustering tendency was observed principally within 60,000 km, although the orbit of HEOS II extends out to 244,000 km. Collection was over a 2-1/2-year period.

(U) The distribution of Figure 7 shows an interesting and dramatic upturn at shorter time intervals. The shortest time interval shown (approximately 0.02 to 0.04 hrs), however, is over 2 orders of magnitude larger than the interval of interest in this analysis. A straightforward extrapolation of the data points in the figure yields a result that is obviously absurd (400,000 detected events). Clearly, the curve must turn down for shorter time intervals, but just how that is accomplished cannot be determined from our current state of knowledge.

(U) A further argument against the applicability of this data is because of the particle mass range of the experiment--10^{-9} gm to 10^{-15} gm. Particles of interest to this analysis are more likely to be 10^{-6} gm or larger.

E. Summary (U)

(U) The principal results of the literature search were:

- The mass-flux curve of Dohnanyi (1972) is substantially correct. However, the Pioneer 10 data indicate that the relationship between the meteoroid flux and optical detections is very complex and not understood at the present time.
- Velocity distribution data for meteors and meteoroids is sparse and unreliable at low velocities because of selection effects that decrease the number of low velocity particles detected. Nevertheless, basic physics dictates that no particles, except for possibly a very few pathological cases, can pass near the spacecraft with relative velocity less than 800 m/sec.
- Expected meteoroid spin rates are so high that glints from specular surfaces should be only microseconds long--not milliseconds.

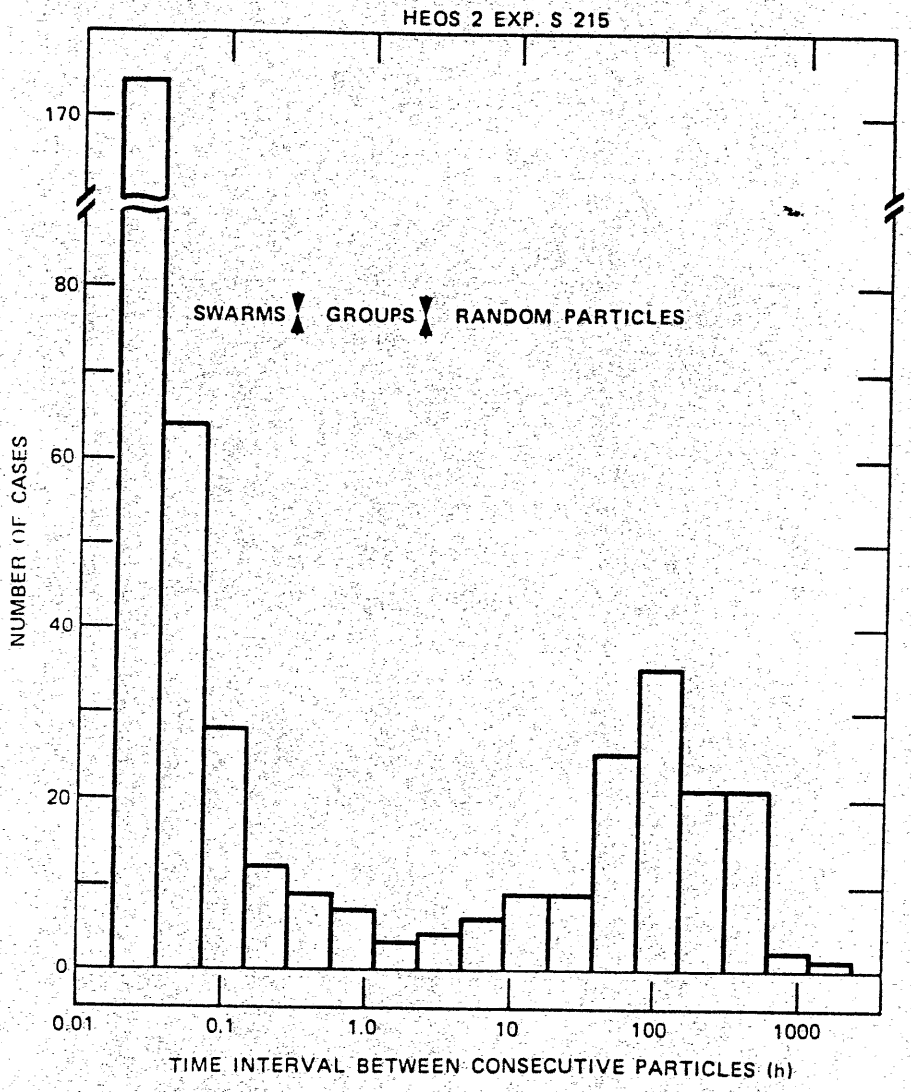

FIGURE 7 NUMBER OF EVENTS AS A FUNCTION OF THE TIME INTERVAL BETWEEN CONSECUTIVE EVENTS (U)

III OPTICAL OBSERVATIONS EXPECTED FROM THE ACCEPTED DATA BASE (U)

(U) Given the particle mass flux statistics described in the previous chapter, it is possible to estimate the frequency of occurrence of events with a peak intensity exceeding any particular level. We shall see subsequently that the available optical experiments differ from the calculated levels. To date, no theoretical model has been proposed that explains the optical observations successfully.

(U) The observations of most interest for this study require both a large peak intensity and a long duration observation. With a complete description of the velocity distribution, the complete bivariate statistical expectation could be calculated. Unfortunately, the long duration events require low velocity particles. These are sufficiently rare that the velocity distribution can be guessed only very crudely. We shall, nonetheless, attempt a calculation.

A. Distribution of Peak Intensity (U)

(U) We assume that the average particle has a scattering function of the form

$$I = I_s \, r \, f(\gamma) \, a^2/R^2 \qquad (1)$$

where I is the scattered intensity, I_s is the solar illumination, r is the reflectivity, $f(\gamma)$ is the scattering phase function, a is the particle radius, and R is the distance from the particle to the optical system. Over a period of time, the phase function will be averaged over a range of angles, γ, that depends on the experimental geometry. For the Pioneer case, a 45-degree deviation from backscatter is typical. For VELA, we assume that all solid angles are equally likely, though this is probably not rigorously true. In the equations that follow, $f(\gamma)$ will not be used explicitly. We shall use

(U)

$$I = K_I \, a^2/R^2 \tag{2}$$

and return later to K_I in particular cases.

(U) The cumulative density of particles with radius a or larger is

$$N(a) = K_N \, a^{-\beta}. \tag{3}$$

The average velocity of the particles normal to any surface is v. Since the system response falls very rapidly outside a cone of half-angle α, the peak intensity in the typical case will occur where the particle enters or exits the cone. If we select a particular distance on the surface of the cone, R, and a particular scattered intensity, I, we can calculate the minimum radius particle needed to produce the desired signal using Equation (2). The number of particles crossing unit area in unit time will then be $N[(I/K_I)^{1/2}R]$. The flux crossing an area element of the cone is

$$dN_I(I) = v \, K_N \, (I/K_I)^{-\beta/2} R^{-\beta} \, 2\pi R \, dR \, \sin(\alpha)$$

$$= \frac{2\pi v \, K_N \, K_I^{\beta/2} \sin(\alpha) \, dR}{I^{\beta/2} \, R^{\beta-1}} . \tag{4}$$

Because of the radius dependence, most events will occur near the lens. The total event frequency can be found by integrating from a minimum distance, R_m, to infinity. A smaller upper limit can be used if appropriate. This integration gives

$$N_I(I) = \frac{2\pi v \, K_N \, K_I^{\beta/2} \sin(\alpha)}{(\beta-2) \, I^{\beta/2} R^{\beta-2}} . \tag{5}$$

(U) Equation (5) indicates that the number of events larger in intensity than I varies as $I^{-\beta/2}$ if the cumulative radius distribution varies as $a^{-\beta}$, provided only that the scattering behavior of the particles is similar for all sizes.

(U) If the particles scatter as Lambert spheres,

$$I = \frac{2\, r\, I_s\, a^2}{3\, \pi\, R^2} (\sin\gamma - \gamma \cos\gamma). \qquad (6)$$

For Pioneer 10, $\gamma = 3\pi/4$, and for VELA it is appropriate to average over all solid angles. Using $I_s = .14$ W/cm^2 and $r = 0.2$, we find

$$K_I = 2.8 \times 10^{-2} \text{ (Pioneer)}$$

$$= 7.0 \times 10^{-3} \text{ (VELA)}.$$

(U) A third, physically unrealistic, model is appropriate for purposes of illustration. Suppose that all particles are hemispheres with a flat, specular surface perfectly oriented to be observed by the Pioneer AMD system. Then

$$I = \frac{2\, r\, I_s \cos^2 (\pi - \gamma)/2}{\pi\theta^2} \frac{a^2}{R^2} \qquad (8)$$

where θ is the angular diameter of the sun. This calculation yields $K_I = 12.57$.

(U) The mass flux distribution (from Dohnanyi, 1972)

$$v\, N(m) = 3.16 \times 10^{-18}\, m^{-1.18} \quad m^{-2}\, s^{-1}\, (2\pi SR)^{-1} \qquad (9)$$

corresponds with a radius distribution

$$v\, N(a) = 5.53 \times 10^{-16}\, a^{-3.54} \quad m^{-2}\, s^{-1}\, (2\pi SR)^{-1} \qquad (10)$$

(U) Estimates of the typical particle density range from 0.18 to 3 gm/cm^3. The numerical values given below assume a density of 3 gm/cm^3 and R_m = 1 m. The estimated number of events of a given intensity can be raised by a factor of 8 by assuming the lowest density estimate. Then we find

$$N_I(I) = 1.08 \times 10^{-17}\ I^{-1.77} \quad \text{Pioneer Lambert spheres}$$

$$= 7.73 \times 10^{-14}\ I^{-1.77} \quad \text{Pioneer specular hemispheres}$$

$$= 3.59 \times 10^{-18}\ I^{-1.77} \quad \text{VELA Lambert spheres}$$

In each case, the value initially calculated has been multiplied by 3.15×10^7 to obtain the number of events per year. For $I = 10^{-8}\ W/cm^2$, N_I is 1.56×10^{-3}, 11.2, and 5.2×10^{-4} events per year for the three cases above, in order.

B. Distribution of Time Durations (U)

(U) The formulas given in the previous section yield the expected frequency of events exceeding a given intensity, regardless of duration. However, we are interested principally in a case where the duration is unusually long. In this case, it is necessary to consider the velocity distribution of particles. Long-lasting meteoroid observations imply low velocities, for which the Pioneer and VELA environments differ significantly. Pioneer acquired data in a region governed entirely by solar gravitation, while the earth's gravity influences VELA. The influence of the earth sets a minimum particle velocity relative to the spacecraft of about 800 m/s for VELA. The only particles that can remain long enough in the field of view to account for very long duration flashes are those with vectors in the principal cone of the field of view. The field of view subtends a solid angle of 2.5×10^{-2} steradians (or 1.9×10^{-3} of the surface area on a sphere of unit radius). Since particles going in either direction are acceptable, only about 3.8×10^{-3} of the incident particles will have velocities in the directions required for a long duration event.

(U) For particles traveling radially outward from the lens, beginning with peak intensity at range R,

$$\frac{I(t)}{I_o} = \frac{R^2}{(R + vt)^2} \tag{11}$$

(U) If extinction occurs when $I/I_o = .01$, $vt = 9\ R$. If we require $v \geq 800$ m/s, $t = .3$ s, then $R \geq 27$ m. More generally, for $t \geq 0.3$ S,

$$R \geq v/30 \tag{12}$$

(U) Consider the case of the Pioneer specular reflectors, which is the physically unrealistic case that yields the largest number of events and comes the closest to the observed Pioneer distribution. Considering only the fraction of particles in the critical cone, we use Equation (5) and the numerical results immediately above to obtain

$$N_c(I) = 2.94 \times 10^{-16}\ I^{-1.77}\ R^{-1.54} \tag{13}$$

The minimum range used in the integration has been reintroduced to be used with the velocity. The number of events of duration t or larger (to .01 of peak intensity) having velocity in the range v to v + dv is

$$dN(I,\ t) = 2.94 \times 10^{-16}\ I^{-1.77}\ (\frac{vt}{9})^{-1.54} f(v)dv \tag{14}$$

An estimate of the velocity distribution for velocities less than about 10 km/s suggests using

$$f(v) = v/8 \times 10^{8} \quad (v \text{ in m/s}) \tag{15}$$

This does not go to zero at v = 800, but the extra events counted will not be numerous. The integral of Equation (14) from 0 to 10 km/s for t = 0.3 s is

$$N(I,\ .3) = 6.21 \times 10^{-26}\ I^{-1.77} \text{ events per year} \tag{16}$$

(U)

For $I = 10^{-8}$ w/cm^2, this yields 9×10^{-12} events per year, or about one event per 10^{11} years. It is interesting to note that this figure is about ten times the currently estimated age of the universe.

(U) The probability calculations above lead one rapidly to the conclusion that there is no possibility that event 747 is meteoroid related. Unfortunately, they also lead rapidly to the conclusion that the observations made by Pioneer 10 are impossible. After a thorough study of the Pioneer 10 AMD experiment, we believe that those data are more relevant to the VELA case than are probability calculations based on other measurements and hypothetical scattering models. These calculations will be used to provide the most intelligent available guide for extrapolation from the Pioneer observations.

IV THE PIONEER 10 AMD EXPERIMENT (U)

(U) The Pioneer 10 AMD (Asteroid/Meteoroid Detector) is strikingly similar in concept to the VELA bhangmeter system. Of all the spaceborne meteoroid experiments to date, it is certainly the most relevant source of data background to indicate the probable VELA meteoroid environment. Unfortunately, the Pioneer 10 data have proved very difficult to relate to other meteoroid data.

(U) Because the Pioneer observations do not relate as expected with other meteoroid observations, it is necessary to consider two alternatives for the use of the Pioneer data:

1. The data are invalid, or
2. Simple optical scattering models are not a proper description of the processes that are responsible for the AMD observations.

After a study of the Pioneer equipment and results, we have concluded that the second alternative is preferable. We believe that the Pioneer data are indicative of the actual optical environment. In this case, the scattering models discussed in the previous chapter must be misleading for some reason. Two suggestions were provided by Dr. R. K. Soberman, the chief investigator for the AMD experiment. The first was that specular glints are a more important mechanism than was initially envisioned. The second was that the electrostatic forces between the spacecraft and passing particles often cause the particles to shatter. The effect would be a sudden expansion to a very large scattering surface for the particle mass.

(U) Specular glints do not appear to offer a very satisfactory explanation of the Pioneer results. The observed distribution of brightnesses and durations cannot be generated even with absurdly

(U)
optimistic descriptions of the specular characteristics of particles. Long-duration specular echoes appear to be extremely improbable because of the large expected rotational speeds.

A. AMD System Description (U)

(U) The AMD consisted of four optical sensors mounted in a square. Each sensor used a reflecting telescope with an 8-inch aperture, and they were mounted with 8½ inches between centers. The field of view was a 7.5° cone, or a half angle of 3.75°. The entire assembly was mounted at 45° to the spacecraft spin axis and pointed in a direction that was generally away from the sun.

(U) The decision logic that determined that an event had occurred required a transient increase in the output of three of the four sensors overlapped in time. The first detector to trigger started four time counters, one for each detector. The time of crossing the threshold was stored for each system and called the "entrance time." When the output fell below the threshold once again, the time was also recorded and called the "exit time." The difference between the entrance and exit times for each channel constitutes the time in the field of view. The peak signal during the time in view was also recorded for each channel.

(U) In principle, the exit and entrance times for objects that transit three detectors can be used to calculate the range and velocity vectors for the particle. The brightness can then be used to determine the size, and the velocity can be summed with the spacecraft velocity to determine the orbit of the particle. In practice, it proved impossible to obtain sensible results from this form of data reduction.

(U) One of the problems with the AMD data may have been electronic. Laboratory experiments showed that electronic cross talk could be responsible for the frequent occurrence of nearly identical entrance times for all AMD sensors. The individual exit time indicators had no restart provision to account for the occasions when a signal fell briefly below the threshold level and subsequently rose above it. The coincidence circuitry did contain restart logic. As a result some events appear from the indicated times not to have three-fold coincidence. Laboratory

(U)
measurements never succeeded in producing events when signals were observed by only two sensors, however.

B. AMD Data (U)

(U) The received data were reduced to a particle size distribution using only the transit-time data. The longest time duration of the t.r. or four indicated observations for each event was a sumed to represent a particle transit close to the center of the field of view. Each particle was assumed to be in circular orbit around the sun, so the velocity relative to the spacecraft could be calculated. With this velocity assumption, the transit time implies a range from the lens. All particles were assumed to be spherical, diffuse reflectors with a reflectivity of 0.2. The known sensitivity of the system then implies that a particle at known range must be a certain minimum size.

(U) Figure 8 shows the particle size distribution derived from this data reduction (Neste, 1974). We have added a power-law fit to the large-size portion of the distribution, which is

$$N(a) = 10^{-21}\ a^{-3} \quad \text{(units are } m^{-3}\text{)} \tag{17}$$

By comparison, the mass flux distribution given by Dohnanyi (1972) can be converted into a particle radius distribution. Using a density of 3 g/cm^3 and an average velocity of 14 km/s, the value is

$$N(a) = 3.29 \times 10^{-27}\ a^{-3.54} \quad (m^{-3}) \tag{18}$$

For meteoroids of 1 mm or larger radius, the respective number densities are

$$10^{-12}\ m^{-3} \text{ and } 1.4 \times 10^{-16}\ m^{-3}.$$

(U) The difference in expected number densities calculated above is also reflected in the calculation of expected event intensities. Following the derivation given in the previous chapter, we find

$$N_I(I) = 8.49 \times 10^{-13} / (R_m I)^{1.5}. \tag{19}$$

For R_m = 1 m, the expected number of events per year exceeding 10^{-8} w/.cm^3 is 0.85.

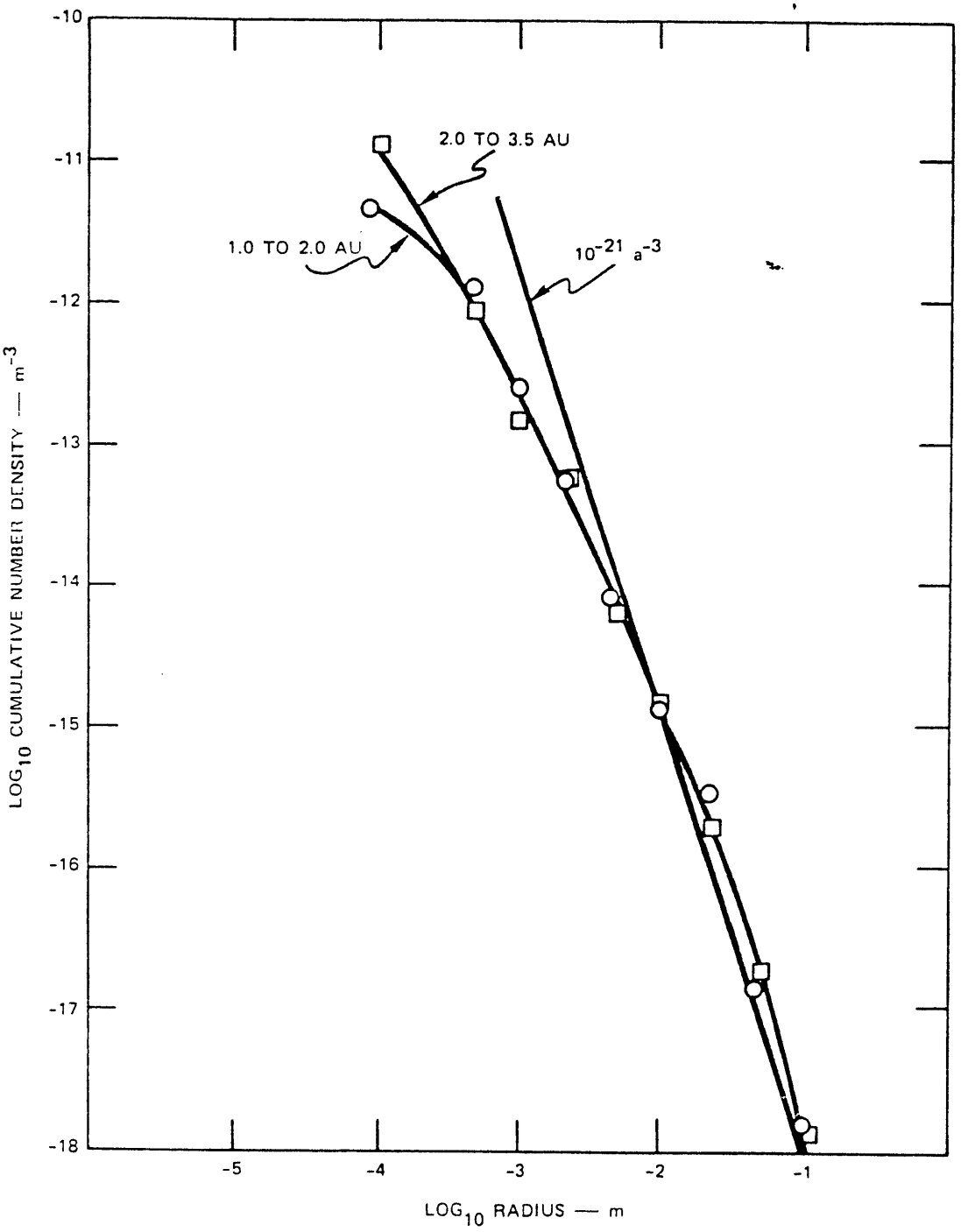

FIGURE 8 CUMULATIVE PARTICLE SIZE DISTRIBUTION DERIVED FROM PIONEER 10 AMD (U)

(U) The measured intensities of the Pioneer events were not used to derive the particle radius distribution. They are available, however, for comparison with the intensity distributions calculated from the mass distribution and from the Pioneer data reduction. Since Pioneer 10 did not remain at 1 AU from the sun, it is appropriate to scale the measured intensities upward by the square of the distance at the time of each measurement. Figure 9 shows the resulting distribution of event intensities. It can be seen that there is little variation in the number of events per half-decade of intensity over the range of the instrument. Because of the scaling with solar distance, neither the lower nor the upper limit is constant for all of the measurements. The unscaled data show sharper cutoffs at both ends.

(U) It is immediately apparent that the number of very bright events, 10^{-8} W/cm^2 or more, is much larger than is given by the above calculation derived from the size distribution obtained from the event time durations. This disparity suggests that the assumptions regarding a uniform scattering law should be questioned. We understand (Soberman, 1980) that there is now underway an attempt to model theoretically the Pioneer results assuming that some of the particles interact with the electric field from the charged spacecraft. These particles may shatter as a result of the added electric stress, producing a much larger reflection than would otherwise be expected on the basis of the particle mass. Such a model would explain the large number of very bright events with respect to the total number of observations.

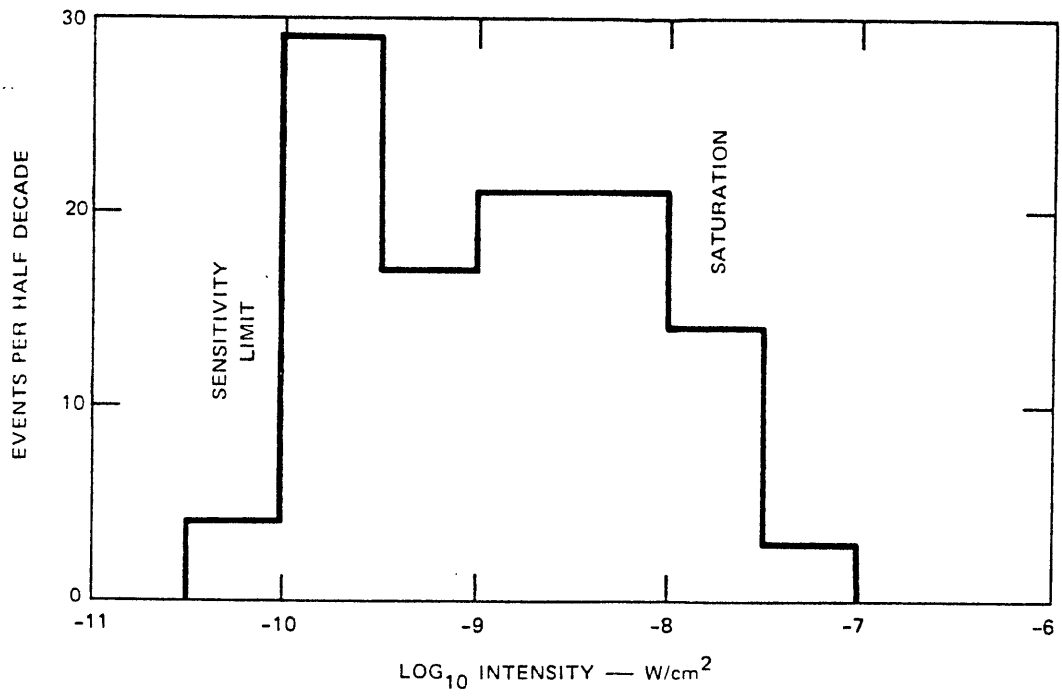

FIGURE 9 DISTRIBUTION OF INTENSITY OF PIONEER 10 EVENTS (U)

V THE VELA "ZOO" (U)

(U) AFTAC has provided us with a set of unexplained VELA observations, generally referred to as the "zoo." The data consist of IBM cards containing the peak intensity, time duration, and energy for a set of events selected by peak amplitude and energy. In addition, we were provided with plots of time histories for most of the events. Another selection criterion was that both YC and YV triggered for all of the events. Data from both instruments were included only if both also met the criteria for amplitude and energy. As a result, about half of the events received contain data for both systems. This underscores one obvious feature of the zoo. It is the exception, rather than the rule, for the two channels to provide consistent data. In some cases, the results are similar enough that it is easy to recognize that the two channels contain related data, but this is not universally the case.

(U) Approximately one-half of the zoo members have time histories for at least one channel that could conceivably be the result of a meteoroid encounter. The best example of this for which we have both YC and YV histories is shown in Figure 10a. These waveforms match almost exactly what one would expect from a diffusely scattering meteoroid passing perpendicular to, and near the center of, the field of view of both sensors. The difference in peak amplitude is the expected 5 LD units.

(U) Figure 10 (a) is an exception, however, even among the time histories that can be labeled "probable meteoroid." Because most meteoroid encounters are expected to be quite close to the spacecraft, it should be common to see differences due to location in the field of view.

(U) Another large class of waveforms in the zoo is exemplified by Figure 10(b). These waveforms are difficult to explain in terms of

THIS PAGE BLANK

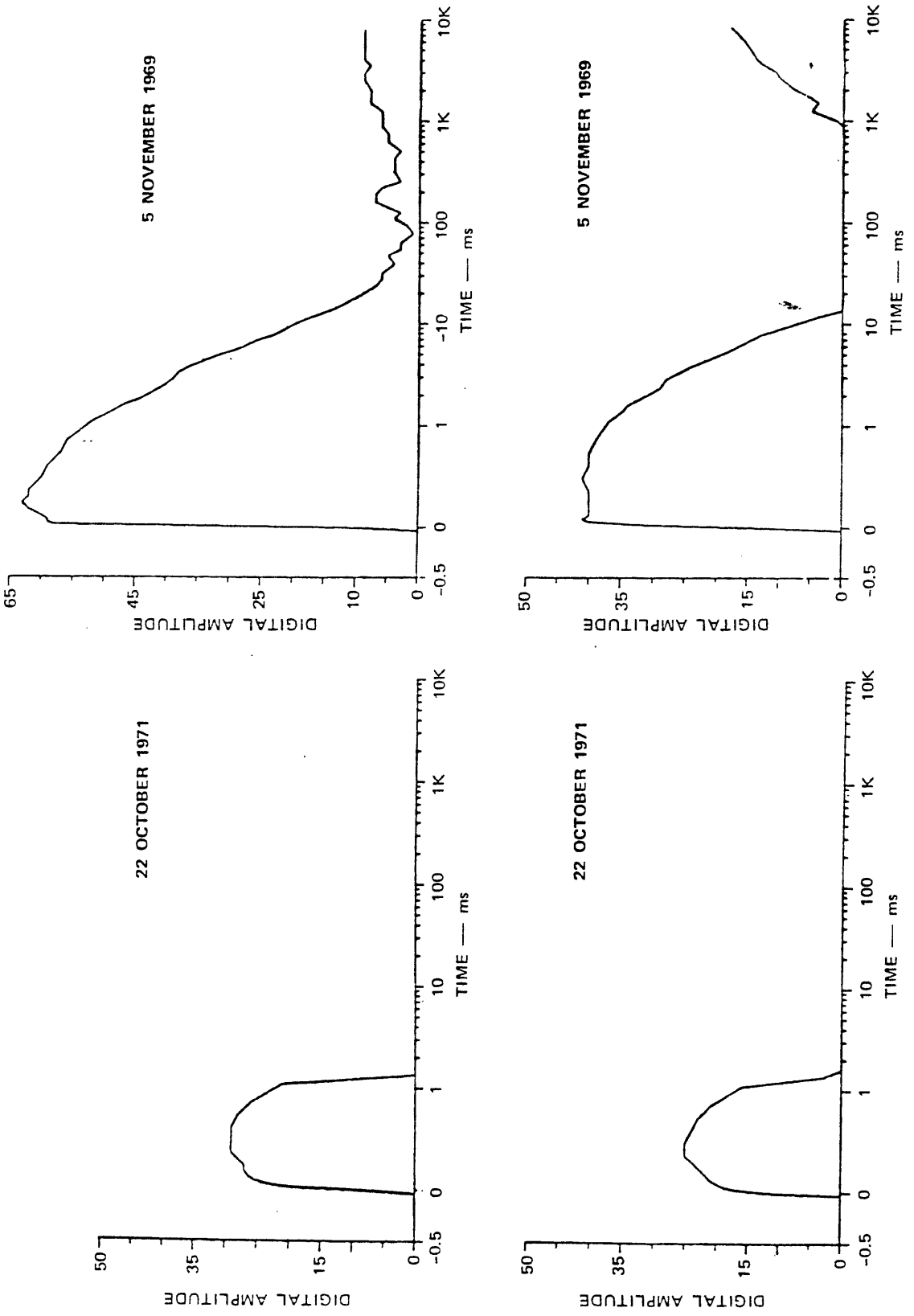

FIGURE 10 SAMPLE MEMBERS OF THE VELA ZOO (U)

(U)
meteoroid encounters, although the reasons are not immediately obvious from a single example. One could postulate a meteoroid trajectory that would explain satisfactorily the time histories shown in Figure 10(b), including the differences between the YC and YV amplitudes. For example, a meteoroid entering the field of view near the lens with a velocity vector that caused it to remain in the field of view as it receded into the distance would account for both the fast rise time and the slow fall time. The anomalously large difference in peak amplitude between the YC and YV sensors might be the result of a trajectory that entered the YC field of view close to that lens and subsequently passed through the YV field of view at a greater distance.

(U) The main difficulty with the above explanation is that there are far too many zoo members with this general shape. If all meteoroid directions are equally probable, less than 1% of the meteoroids should fall into the cone where the rise time is much, much less than the decay time. It is very difficult to account for the large number of these waveforms in this way. This conclusion should be tempered, however, by consideration of the selection process involved in obtaining the zoo. The requirement for signals with large energy might be an effective way to screen out most bright meteoroids that do not fall into the long-duration viewing cone. The other 99% may have been observed and rejected as uninteresting signals.

(U) The time histories expected for diffusely reflecting meteoroids are relatively easy to predict. The Pioneer 10 results suggest that specular glints should be common, and these are a bit more difficult to recognize with any certainty. For nearby meteoroids, large differences between the sensor outputs would not be surprising. The theoretically-expected high rotation rates for meteoroids suggest that specular glints should often be shorter than the 30-μs sampling interval. Such glints might be the cause of some of the very fast observed rise times in the VELA zoo, but we would expect the fall time to be rapid also. Presumably, the fall time would be determined by the 5-kHz filter circuit used during the early part of the time history sampling.

(U) In summary, from an examination of the VELA zoo time histories, we believe that a substantial fraction of the zoo can be attributed to meteoroid encounters. In the following section, the zoo and AMD data are compared on the basis of similar information. This comparison also leads to the conclusion that it is unlikely that all of the VELA zoo can be attributed to a meteoroid environment like that of Pioneer 10.

VI COMPARISON OF PIONEER 10 DATA WITH VELA "ZOO" (U)

(U) Figure 11 shows the conversion from digital amplitude units to optical intensity for both the AMD and the VELA YC detectors. While the Pioneer detector is significantly more sensitive, there is a useful range of overlap between the two systems. It is particularly interesting that the AMD system saturates at an amplitude roughly equal to the peak of the 747 event.

(U) To confine the data analysis to a region that is roughly comparable with the environment of the earth, we chose to analyze only the 109 events observed during the 124 days of operation between 1 and 2 AU from the sun. Peak intensity observations were normalized to 1 AU using

$$I = I_o S^2 \qquad (20)$$

where I is the normalized intensity, I_o the observed intensity, and S is the distance to the sun, measured in AU.

(U) Signature duration statistics were compiled using the largest of the four AMD time durations, the same procedure used by Soberman and Neste (1974). Neste mentions that simulations of the AMD operation conducted during the flight uncovered a problem with electronic cross talk that frequently resulted in all entrance times being set to zero or a small value. Some of the data must, therefore, be biased slightly toward larger times than were actually observed. A contrary bias, also in the electronics, was the lack of a restart feature on the exit timers to count the full signature duration if there was a momentary dropout while the particle was in the field of view. This situation might be produced by a particle with specular facets as it rotated while crossing the field of view.

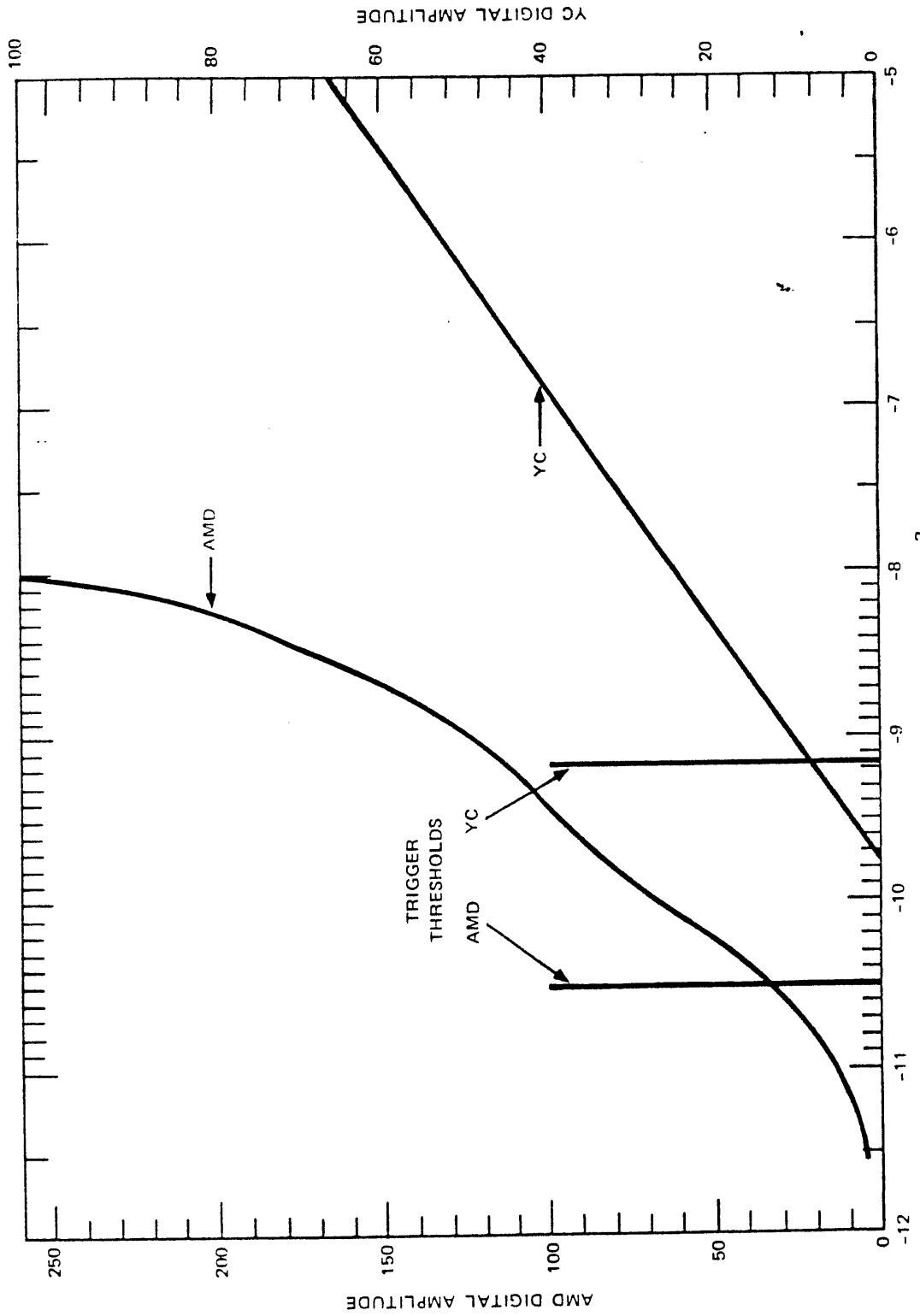

FIGURE 11 DIGITAL OUTPUT VALUES vs. INTENSITY FOR THE AMD AND YC DETECTORS (U)

(U) We processed the data from the VELA zoo events to simulate the AMD results so that the two data sets could be compared. This processing consisted of selecting the larger of the YC and YV peak amplitude and time duration values from the figures scaled by AFTAC. This selection reduced each pair of values in the zoo to a single event, with the scaling performed as if the sensors were part of the AMD experiment. After the selection process was completed, there were 83 events, taken from a sample period of about 22.8 sensor-years. The intensity and duration figures from these events have been converted to an events-per-year basis for comparison with the Pioneer 10 data. The results are shown in Figures 12 and 13.

(U) The Pioneer 10 intensity data shown in Figure 12 do not show a trend that provides a clear basis for extrapolation to larger intensities. With no clear trend of the data, we must resort to the only available physical model to provide an indication of what to expect. The specular reflector model used in Chapter III gives the cumulative distribution shown by the sloping line. A similar power-law extrapolation from the largest Pioneer 10 intensity makes it difficult to account for the most intense of the VELA events.

(U) The power-law extrapolation from the Pioneer results is, however, only a guess at the most reasonable form of extrapolation. Pioneer 10 obtained several bright, long-duration echoes around 1.2 AU--near the earth. On the basis of this limited sampling, one could also speculate that the environment near the earth's orbit may differ significantly from that near 2 AU. On balance, however, it is difficult to account for the very brightest of the VELA zoo events in terms of meteoroid encounters.

(U) Figure 13 shows that an extrapolation of the brightest of the AMD events to longer durations indicates that the VELA zoo and event 747 fit quite reasonably. The longest Pioneer 10 observation lasted about 38 ms, and the observing period was about four months. Extrapolating as t^{-1} (suggested by Figure 13) or $t^{-1.5}$ (suggested by Equation 14) indicates that a bright event lasting 390 ms might be expected at intervals of 3 to 10 years.

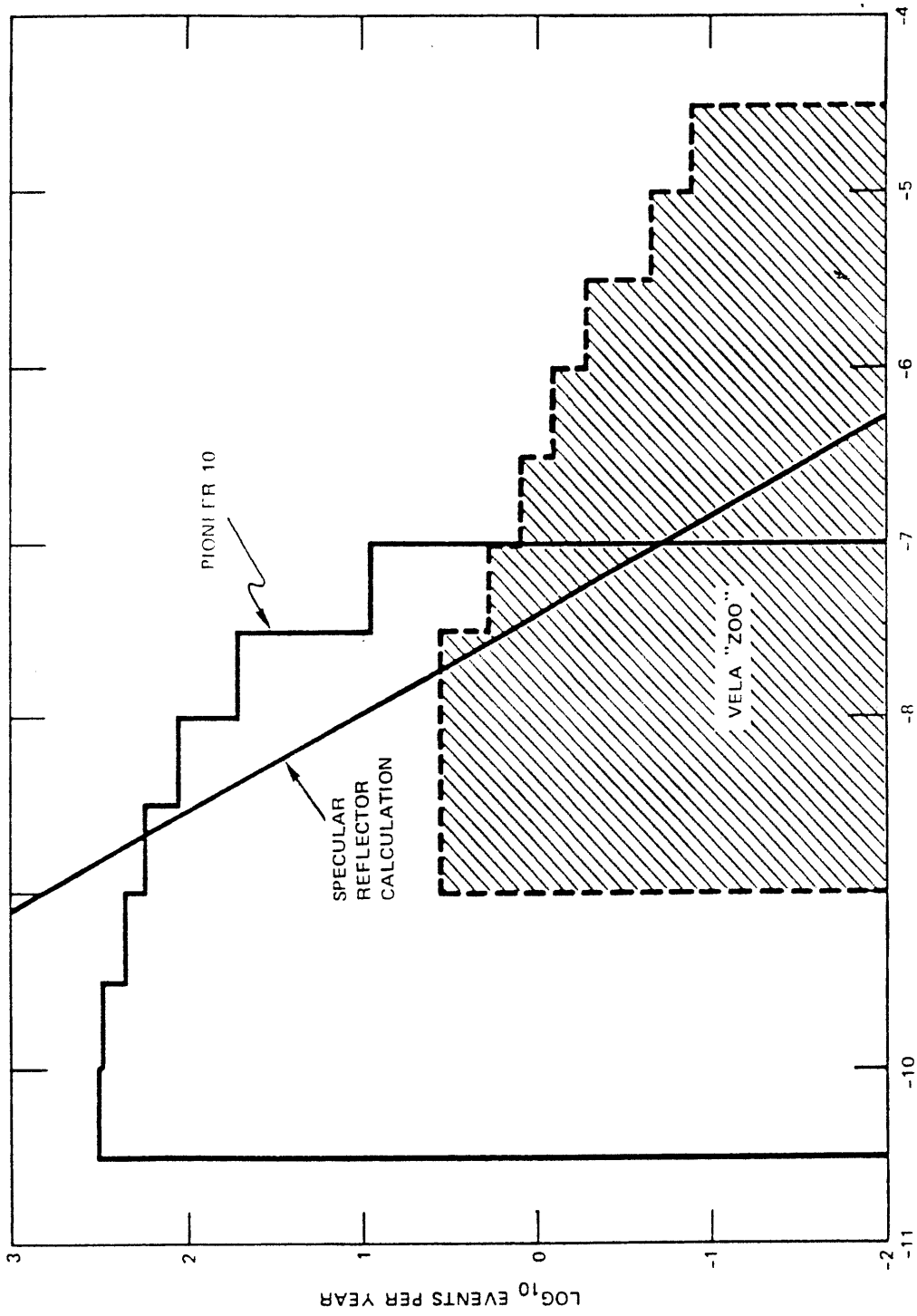

FIGURE 12 CUMULATIVE INTENSITY DISTRIBUTIONS FOR PIONEER 10 AND THE VELA ZOO (U)

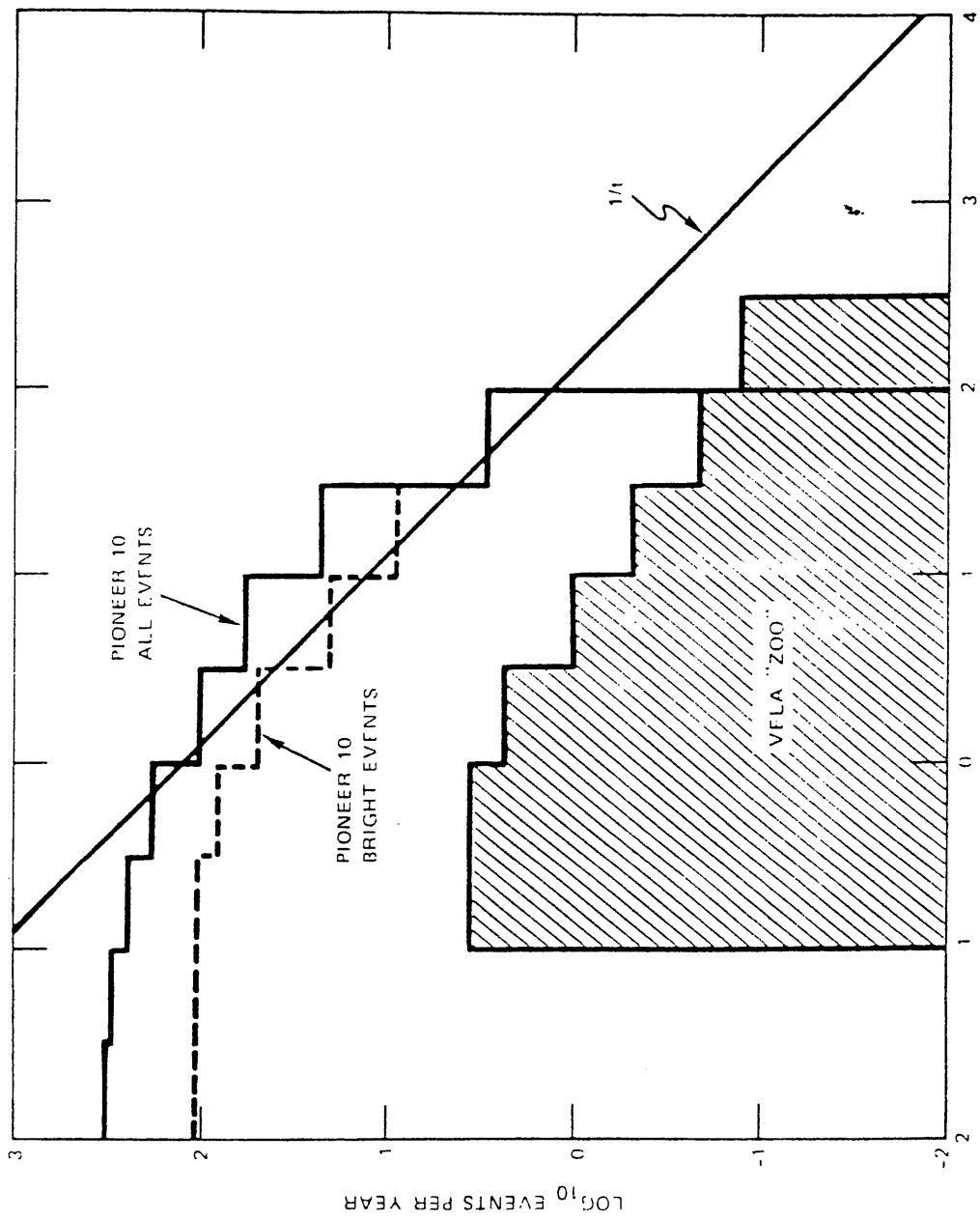

FIGURE 13 CUMULATIVE DURATION DISTRIBUTIONS FOR PIONEER 10 AND THE VELA ZOO (U)

(U) The difference between the Pioneer 10 and VELA gravitational environments may have an impact on the probability of long-duration events. The primary population of interplanetary particles cannot encounter VELA with a relative velocity less than about 800 m/s. Experiments such as HEOS II (Fechtig, et al., 1979) indicate that the secondary population of particles affected by earth encounter is confined within about ten earth radii, or well within the VELA orbit. Although encounters with extremely low velocity particles are rare in any case, they may be sufficiently more probable for Pioneer to bias the data shown in Figure 13 somewhat in favor of long-duration events.

VII CONCLUSIONS (U)

(S) The problems posed at the outset of this study consisted of a literature search, a comparison of Pioneer 10 and VELA data, and the evaluation of two, specific physical models that might generate the Event 747 signature. The first two items have been addressed as intended. The study of the Pioneer 10 results leads to the inescapable conclusion that the two physical models were based on a conception of the optical signal generation process that is not compatible with the Pioneer 10 data. Accordingly, these particular physical models are improbable in the extreme, but they clearly do not exhaust the possible mechanisms for generation of the 747 signal.

A. Results of the Literature Search (U)

(U) The literature search reveals a large number of experiments relating to the flux of meteoroids of varying masses. The results of these experiments exhibit a consistent trend over an enormous mass range. Data on meteoroid velocity distributions are much more sparse, particularly at the low-velocity end of the distribution curve. The rotation of small meteoroids has only been discussed theoretically. Theory indicates that the typical small particle should be rotating at speeds of the order of 10^5 or more revolutions per second.

(U) Pioneer 10 stands out as a unique meteoroid experiment that is very difficult to relate to the other data. The problem appears to be one of interpretation, not of invalid data. As a result, we consider the Pioneer 10 data to provide the best data base to relate to VELA.

B. The MRC Model (U)

(U) The MRC model consists of an approximately hemispherical particle crossing the optical axis at a range of a few meters and at a

(U)

speed of a few m/s. We have not addressed the problem of the shape and orientation of this particle, because it is not an allowable component of the meteoroid environment. Such a particle might be generated by impact with the spacecraft, or by some other local process. The MRC team decided, however, that it is difficult to conceive of a mechanism that would drive a locally-generated particle into the correct trajectory.

C. The Sandia Model (U)

(S) The Sandia model consists of two, independent meteoroids, each generating one of the maxima of the Event 747 signal. Using the meteoroid flux model obtained from the literature search, we calculate that the probable frequency of single meteoroid observations with the same peak intensity and duration as Event 747, with no additional constraints, is one per 10^{11} years. This result, however, is clearly not in agreement with the implications of the Pioneer 10 data.

(S) A two-meteoroid model cannot be supported by the most optimistic view of the Pioneer data. The Pioneer data suggest that a signal comparable with the first 747 pulse will be obtained on the order of 10 times per year (see Figure 13). There is neither a physical argument nor a clear enough trend in the Pioneer data for confident extrapolation to pulses that might match the second 747 pulse. The most optimistic estimate we can conceive of is that such an observation might occur every 3 years (compare with 10^{11} years). The HEOS II data (Fechtig, et al., 1979) indicate that swarms of meteoroids are common within 60,000 km of the earth, but rare outside that limit. Thus, the best model appears to be that the two meteoroids are independent. In this case the probability that a long pulse would be accompanied within 10 ms by a short one to produce a 747-like event is 3×10^{-9}. Since long-pulse events are not expected to occur more often than once each three years, we can expect to wait about 10^{9} years for a suitable coincidence.

D. Comparison of Pioneer 10 and VELA (U)

(U) It is very probable that there is a substantial overlap between the Pioneer 10 and VELA zoo observations. Saturation of the Pioneer 10 detectors on several occasions makes it impossible to use the existing data as a satisfactory basis for extrapolation to determine the probable frequency of very bright events. The only physical model we have is demonstrably inadequate to explain the Pioneer observations, so it also provides a weak basis for extrapolation. We are left with a mostly subjective conclusion that VELA observes extremely bright events too often to be attributed to the same mechanism as the Pioneer 10 data. On this basis, we doubt that all of the VELA zoo events can be attributed to the same cause as the Pioneer 10 data.

(S) The Pioneer 10 AMD provided no time histories. This omission is crucial for the evaluation of Event 747, because we do not know whether any of the AMD observations resembled either a puzzling portion of the VELA zoo or the 747 time history. The VELA zoo contains a large number of events with fast rise times and slow decay times. Perhaps these are examples that support the bursting particle hypothesis for the Pioneer 10 results. The VELA zoo also contains a number of time histories with two maxima. Since it is impossible to compare with Pioneer 10, we cannot evaluate whether these time histories originate from meteoroids, or from some other cause.

(U) In the critical realm of time histories, the VELA zoo must stand by itself as a body of observations that constitute the VELA noise background. Whatever the physical cause, these are the observations that have been reported by the system in the almost 23 spacecraft years of data that were searched.

E. Summary (U)

(S) In the limited time available for this study, we have not been able to reach a firm conclusion regarding the probability that Event 747 was produced by a meteoroid encounter. The best available relevant data base outside of the VELA observations is that of Pioneer 10. The

(S)

evidence provided by Pioneer 10 indicates that the extremely improbable situations envisioned in the MRC and Sandia models do not exhaust the possible means for producing optical signals from meteoroids. Because there are no time histories from the Pioneer 10 experiment, it does not contain sufficient information on which to base a decision.

(S) We are forced to conclude that the only truly relevant data base is that produced by the VELA spacecraft. Whatever the physical cause of each event, this substantial body of observations contains a description of the spacecraft environment as it is viewed by the optical sensors.

(S) The VELA "zoo" is the product of an extensive search of the data base in the attempt to locate events similar to Event 747. As a potential member of the zoo, Event 747 has some very unusual properties. The rise time is exceptionally slow. Events with two maxima are unusual. Events with both the amplitude and duration of Event 747 are also unusual. The probability that all of these properties will occur simultaneously can be estimated from the data base. This effort is beyond the scope of the current study.

REFERENCES (U)

Auer, Siegfried (1976), "Comment on the composition of Soberman particulates in the asteroid belt," J. Geophys. Res., 81, p. 3477-3478.

Bedford, D.K., Adams, N.G., and Smith, D., (1975), "The flux and spatial distribution of micrometeoroids in the near-earth environment," Planet. Space Sci., 23, pp. 1451-1456.

Brownlee, D.E., (1979), "Interplanetary dust," Rev. Geophy. and Space Phy., 17, pp. 1735-1743.

Cook, A.F., (1978), "Albedos and size distribution of meteoroids from 0.3 to 4.8 AU," Icarus, 33, pp. 349-360.

Dohnanyi, J.S., (1972), "Interplanetary objects in review: statistics of their masses and dynamics," Icarus, 79, pp. 1-48.

Dohnanyi, J.S., (1978), "Particle Dynamics," in Cosmic Dust, J.A.M. McDonnell, ed., Wiley Interscience, Chichester, 1978.

Duennebier, F., and Sutton, G.H., (1974), "Meteoroid impacts recorded by the short-period component of Apollo 14 lunar passive seismic station," J. Geophys. Res., 79, 4365-4374.

Fechtig, H., Grün, E., and Morfill, G., (1979), "Micrometeoroids within ten Earth radii," Planet. Space Sci., 27, pp. 511-522.

Gerloff, U., and Berg, I.E., (1972). Preprint, XVth COSPAR meeting, Madrid.

Hoffman, H.J., Fechtig, H., Grün, E., and Kissel, J., (1975), "First results of the micrometeoroid experiment S215 on the HEOS 2 satellite," Planet. Space Sci., 23, pp. 215-224.

Hoffman, H.J., Fechtig, H., Grün, E., Kissel, J., (1975), "Temporal fluctuations and anisotropy of the micrometeoroid flux in the earth-moon system measured by HEOS 2," Planet. Space Sci., 23, pp. 985-992.

Hughes, David (1978), "Meteors," in Cosmic Dust, J.A.M. McDonnell, ed., Wiley Interscience, Chichester, 1978.

Humes, D.H., Alaverez, J.M., O'Neal, R.L., and Kinard, W.H., (1974), "The interplanetary and near-Jupiter meteoroid environments," J. Geophys. Res., 79, pp. 3677-3684.

Latham, G.V., Ewing, M., Press, F., Sutton, G., Dorman, J., Nakamura, Y., Toksoz, N., Lammlein, D., and Duennebier, F., (197-), "Passive seismic experiment," Apollo 16 Preliminary Science Report, NASA, SP-315, pp. 9-1 to 9-29.

Mauth, G.H., (December 1979), "Vela Meteoroid Model," Sandia Laboratories, Albuquerque, NM 87115

Mauth, G.H., (January 1980) letter to Seiler, L.W., and Van Workum, J.A.

McDonnell, J.A.M., (1978), "Microparticle studies by space instrumentation," Cosmic Dust, J.A.M. McDonnell, ed., Wiley Interscience, Chichester, 1978.

Neste, Sherman L., (1974), "An experimental model of the asteroid/meteoroid environment from 1.0 to 3.5 AU - its characteristics and implications," Ph.D. Thesis, published in the Technical Information Series, No. 74SD241, General Electric Space Division.

Paddock, S.J., and Rhee, J.W., (1976), "Rotational bursting of interplanetary dust particles," Lecture Notes in Physics 48, Elsässer and Fechtig, eds., Springer-Verlag, Berlin 1976.

Radzievsky, V.V. (1954), "A Mechanism of the disintegration of asteroids and meteoroids," Dokl. Akad. Nauk, SSSR, 97, 49-52.

Sappenfield, D.S., Sowle, D.H., and McCartor, T.H., (December 1979), "Possible origins of event 747 optical data (U)," Mission Research Corporation, Report MRC-79-443, Santa Barbara, CA 93102, SECRET

Soberman, R.K. Neste, S.L., and Lichtenfeld, K., (1974), "Optical measurement of interplanetary particulates from Pioneer 10," J. Geophys. Res., 79, pp. 3685-3694.

Soberman, R.K., (1975), "Reply," J. Geophys. Res., 81, pp. 3479-3480.

Soberman, R.K., (1980), "Verbal communication," NASA Ames Research, January 1980.

Southworth, R.B., and Sekanina, Z., (1973), "Physical and dynamical studies of meteor," NASA Cr-2316.

Wolf, H., Rhee, J.W., and Berg, O.E., (1976), "Orbital elements of dust particles intercepted by Pioneers 8 and 9," Lecture Notes in Physics 48, Elsässer and Fechtig, eds., Springer-Verlag, Berlin, 1976.

Zook, H.A., and Berg, O.E., (1975), "A source for hyperbolic cosmic dust particles," Planet Space Sci., 23, pp. 183-203.